proceedings

MDPI

Proceedings

Efficient and Eco-Friendly Mechanical Milling Preparation of Anatase/Rutile TiO_2-Glucose Composite with Energy Gap Enhancement †

Imane Ellouzi [1,*] and Hicham Abou Oualid [2,*]

[1] Faculty of Sciences, University Mohammed V, Rabat, 4 Avenue Ibn Battouta, Rabat B.P. 1014 RP, Morocco
[2] Faculty of Sciences and Technologies, University Hassan II of Casablanca, Mohamedia, B. P. 146, 20650 Mohammedia, Morocco; hicham.abououalid@gmail.com
* Correspondence: im.ellouzi@gmail.com (I.E.); hicham.abououalid@gmail.com (H.A.O.); Tel.: +212-66-777-2424 (H.A.O.)
† Presented at the 1st International Online Conference on Nanomaterials, 1–15 September 2018; Available online: https://iocn-2018-1.sciforum.net/.

Published: 4 September 2018

Abstract: In the current study, Anatase/rutile TiO_2 and Anatase/rutile TiO_2@Glucose composites were successfully prepared by a simple method using mechanical technique. The as-prepared composite materials powders were characterized by Powder X-ray diffraction analysis (PXRD), Scanning electronic microscopy (SEM), and Solid-state UV-visible spectroscopy. X-ray patterns showed the fractional phase transformation from TiO_2 anatase to rutile. SEM observations revealed that the particle shape was affected by the ball milling process. Energy-dispersive X-ray spectroscopy (EDS) analysis exhibits quantitatively the elemental composition of Ti and O. UV-Visible spectroscopy confirmed that the bandgap is slightly affected using Tauc.

Keywords: anatase/rutile; composite; TiO_2; mechanical technique; TiO_2-Glucose and gap energy

1. Introduction

Titanium dioxide (TiO_2) is among the most useful materials for many applications due to its nontoxicity, low cost, physical and chemical stability, availability, and optical properties [1]. Titanium dioxide (TiO_2) exists as three different phases; anatase, rutile, and brookite [2]. The band gaps (3–3.2 eV) of TiO_2 semiconductors, absorb just from the UV region of the solar spectrum. Several processing techniques have been used to synthesize TiO_2 particles, coprecipitation [3], and sol-gel [4], etc. Among these methods, high energy milling is an effective and general term describing mechanical action by hard surfaces on a material and it has the advantages to break up the particles and reduce their particle size, simple, and easy. The effect of various ball milling parameters on the properties of the bulk samples, relatively inexpensive, and applicable to any class of materials, Ball milling is applicable to any class of materials and relatively inexpensive and has an effect on the properties of the bulk samples, which can be easily scaled up to large quantities [5]. Ball milling has attracted considerable attention and it is an effective physical mechanical milling synthesis method, owing to the relatively low installation cost, the large number of particles that can be easily obtained by solely grinding bulk materials in a milling vessel with milling balls, and the capability to treat materials of all hardness degrees. However, few studies have been reported on the production of TiO_2 particles by ball milling [6–16]. The milling is a simple and an easy method for increasing the particle size from macro to nanometric level. In addition, ball milling is one of the effective mechanical milling processes and the milling time plays very important role. During ball milling, many parameters could be studied to decrease the particles size, such as the powder-to-ball weight ratio, high speed

rotating grinding machine, and time of mechanical process [17]. The purpose of this work is to modify the particles size and shape, crystal structure, optical properties, as well as phase transformation of TiO_2 using high energy ball milling process. We have also investigated the effect of Glucose on the morphological and optical properties of milled anatase-rutile TiO_2 composites, as well as the gap energy of as-prepared composite materials.

2. Materials and Methods

2.1. Materials and Reagents

TiO_2 powder and glucose were purchased from Aldrich and were used without any further purification. Commercial TiO_2 (TiO_2_C) powders with an average crystallite size of about 134 nm was used as precursor. Ball milling (BM) was carried out using a high energy planetary ball mill machine (Retsch PM100, Haan, Germany).

2.2. Synthesis Procedure

All of the milled samples followed the same experiment conditions: revolution speed fixed at 450 rpm; room temperature; and, stopped periodically for every 30 min and then resumed for 30 min. The milling time period was 2 h and the mass ratio of stainless steel balls to TiO_2 was set at 20:1. After ball milling process, the color of TiO_2 powders has become gray-blue. The changed of color from yellow to gray could be explained by the fact that TiO_2 got its proper structure of its oxide phase. Gray color after calcination is unchanged, which confirms that the powders were not contaminated (incorporation of zirconia or other impurity). Furthermore, the color change is from reduction (formation of oxygen vacancies), which was proved by Energy-dispersive X-ray spectroscopy (EDS). Thus, the color comes from the material itself. Subsequently, 1 g of glucose was dissolved in deionized water and agitated until miscibility and then added dropwise into milled TiO_2 solution and aged all night. At the end of the reaction, the final products were filtered and washed with deionized water, ethanol, and then dried at 80 °C for 24 h in a vacuum oven to give TiO_2-M@G composite (Figure 1).

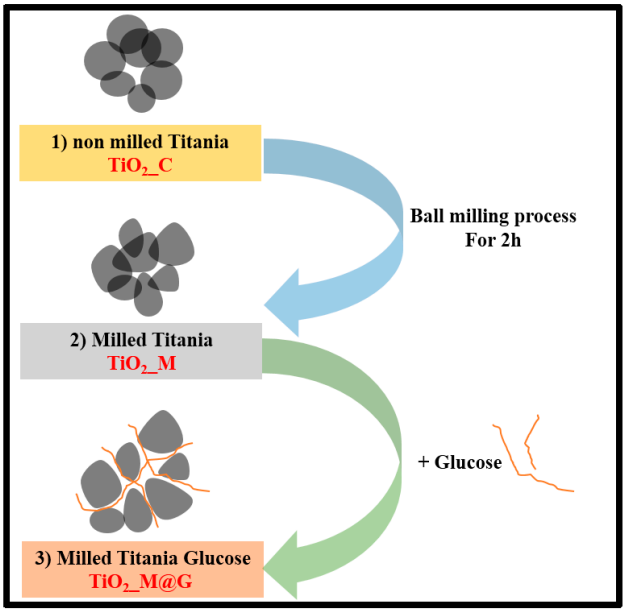

Figure 1. Schematic illustration of synthetic chemical process of composite materials.

2.3. Characterizations and Techniques

Powder X-ray diffraction (PXRD) patterns were obtained at room temperature on a Bruker AXS D-8 diffractometer using Cu-Kα radiation in Bragg-Brentano geometry (θ–2θ). The Scanning

electronic microscopy (SEM) and EDS analysis was recorded by (JEOLJSM-IT100, Japan) with gold sputter coating (JEOL Smart Coater, Japan). The UV–vis diffuse reflectance spectrum was obtained while using Perkin-Elmer Lambda 35 UV-Visible spectrophotometer.

3. Results and Discussion

Figure 2 displays the comparison of XRD patterns of pure anatase (TiO_2-C), milled TiO_2 (TiO_2-M), and milled TiO_2@Glucose (TiO_2-M@G). The major reflections of non-milled material (TiO_2-C) exhibits a major peak at 2θ value of 25.3°, 37.8°, 48.0°, 53.7°, 54.9°, and 62.5°, which corresponds to anatase (1 0 1), (0 0 4), (2 0 0), (1 0 5), (2 1 1), and (2 0 4) crystal planes (JCPDS 21-1272), respectively. Figure 2b,c exhibit diffraction peaks at 2θ of 25.2°, 27.2°, 35.9°, 37.8°, 41.2°, 47.8°, 54.2°, 55.2°, and 62.4°, which can be indexed to the TiO_2 anatase and rutile composite. This result indicates that there is a phase transformation during the milling from anatase to rutile. It could be assigned to the enormous amount of heat induced by high energy, which if not controlled could thermally transform anatase to rutile phase or to the difference in speeds between the balls and grinding jars, which could produce an interaction between frictional and impact forces, releasing high dynamic energies [18].

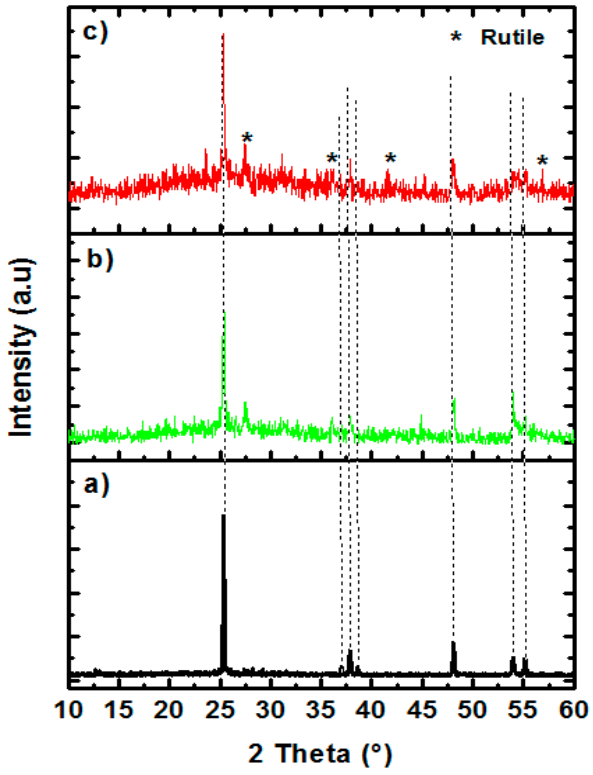

Figure 2. Powder X-ray diffraction (PXRD) patterns analysis of pure anatase (TiO_2-C) (**a**), milled titanium dioxide (TiO_2-M) (**b**), and milled TiO_2@Glucose (TiO_2-M@G) (**c**).

A decrease was observed in the intensity of the Bragg peak of the crystalline phase, while a broad, amorphous phase signal emerged for milled samples. A decrease in the intensities of peaks that was observed could be due to the decrease in the grain size and lattice distortion. These effects could be assigned to the change in the particle size and internal structure of TiO_2 crystallite induced by the ball milling process. It has been reported by some authors that the increase in lattice strain and the reductions in crystallite size could be assigned to the peak broadening [19–21].

The comparison of SEM micrographs and the corresponding EDS microanalysis of pure TiO_2-C and TiO_2-M, TiO_2-M@G composites at 4000× are presented in Figure 3a–c, respectively. It was found that the milling process does not change the morphology of powders as well as the agglomeration of small particles. It is confirmed by particle size distribution, presented in the insets of Figure 3a,b, that the mean particle size of the milled sample (~108 nm) is much smaller than that of TiO_2_C without

milling (~143 nm). The micrographs illustrate that the particles have unequal sizes and they do not have a well-defined geometric morphology.

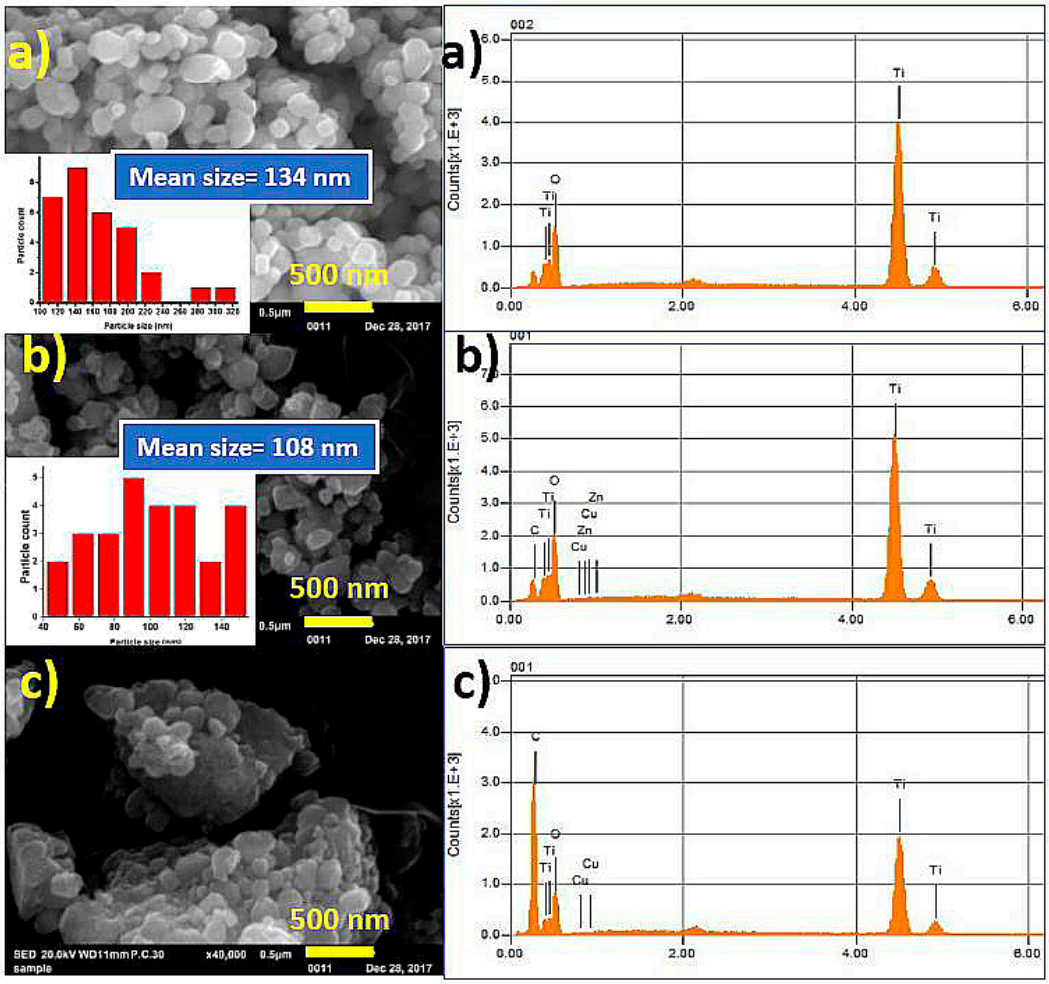

Figure 3. Scanning electronic microscopy (SEM) images and Energy-dispersive X-ray spectroscopy (EDS) analysis of TiO_2-C (**a**), TiO_2-M (**b**), and TiO_2-M@G (**c**).

The composition of TiO_2_C, TiO_2_M, and TiO_2_M@G powders exhibits the lowest amount of oxygen (Ti:O ratio of 0.84), followed by TiO_2_M and then TiO_2_M@G (Ti:O ratio of 0.89–3.94 and 0.62–0.56, respectively). The EDS analysis does not show the presence of zirconia, which confirms that the change of color (grey) is induced from oxygen vacancies and not from ball milling contamination. The high energy that is produced from ball milling in planetary ball mill produced from the collisions between balls and container wall has an influence on TiO_2 powders. In addition, it could create some defects into TiO_2 structure. These defects and the interaction between neighboring crystallites at higher strains, thereby resulting in a smaller crystallite size [22–24]. During annealing, Ti could be reduced into Ti_3O_5 (Ti_nO_{2n-1}), which are based on rutile with oxygen vacancies or into TiO_x where $x < 2$ a mixed oxide of titanium.

Figure 4A,B exhibits the solid-state UV-Visible absorption spectra of TiO_2-C, TiO_2-M, and TiO_2-M@G in the range of 200–800 nm and the corresponding Tauc plots, respectively. A small enhanced absorption was observed in the range of 350–800 nm. The absorption peak of TiO_2-C was located at 312 nm, somewhat red-shifted for both TiO_2-M and TiO_2-M@G composite materials. Contrary to Dulian et al. [25], they reported that the increase of the absorbance of TiO_2 in the visible light is related to the addition of methanol in ball milling process. The band gaps extracted by plotting $(\alpha h\upsilon)^{1/2}$ versus photon energy ($h\upsilon$) using Tauc plot for pure TiO_2-C, TiO_2-M, and TiO_2-M@G composite materials are presented in Figure 4.

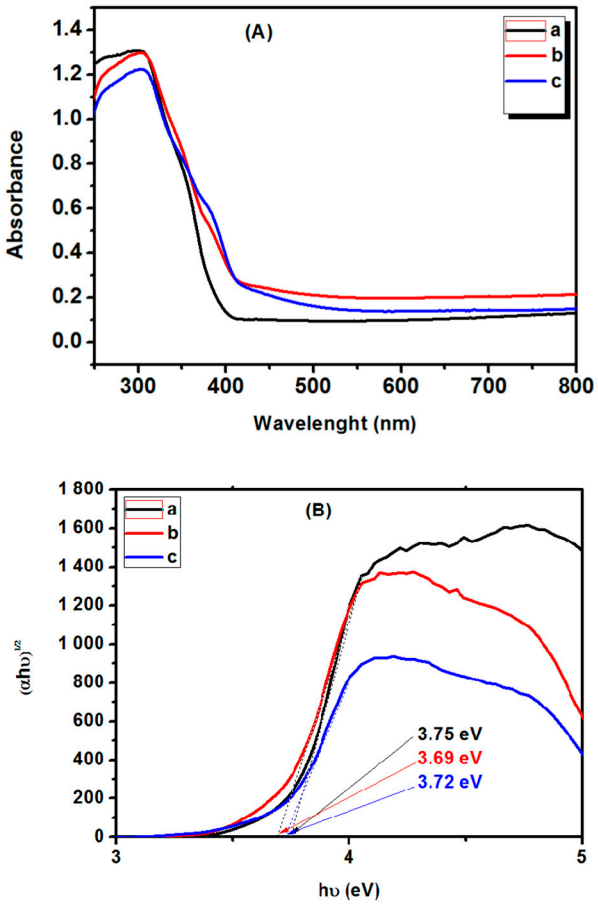

Figure 4. (**A**) UV-Visible absorbance and (**B**) Tauc plot of TiO_2-C (**a**), TiO_2-M (**b**), and TiO_2-M@G (**c**).

The measured bandgap for pure TiO_2 anatase was about ~3.2 eV, which agrees with the literature value [26]. The appearance different band energies for TiO_2-C, TiO_2-M, and TiO_2-M@G composite materials demonstrated the nature of the synthesized materials. Furthermore, as compared to pure TiO_2-C, a slight red-shift of ~0.07 and ~0.03 eV in the band edge position of TiO_2-M and TiO_2-M@G composite materials was observed, respectively. In the case of TiO_2-M, the influence of the ball milling process transformed partially the TiO_2 anatase to rutile phase is the credible reason for this effect. The high speed generated from grinding could increase the temperature and promote the reduction of TiO_2. The vacancy state turns as Ti^{3+} and or Ti^{4+} and it creates new energy level just below the conduction band of the material [27].

4. Conclusions

In this paper, we have prepared anatase/rutile TiO_2 composite and anatase/rutile TiO_2@glucose composite using the high energy ball milling process. This method could be a very efficient and leads to a decrease of particle size, phase transformation of TiO_2 partially from anatase to rutile, and the absorption in the visible light. The suggested process is cost effective, ecofriendly, and it could be applied to prepare composites containing anatase-rutile TiO_2 and anatase-rutile TiO_2-glucose.

Conflicts of Interest: We declare that this manuscript is original, has not been reported before, and is not currently being considered elsewhere. We also confirm that there is no known conflict of interest regarding this manuscript and its publication. The manuscript has been approved by all named authors.

References

1. Wang, Y.; Sun, C.; Zhao, X.; Cui, B.; Zeng, Z.; Wang, A.; Liu, G.; Cui, H. The Application of Nano-TiO_2 Photo Semiconductors in Agriculture. *Nanoscale Res. Lett.* **2016**, *11*, 529–535.
2. Zhang, J.; Zhou, P.; Liu, J.; Yu, J. New understanding of the difference of photocatalytic activity among anatase, rutile and brookite TiO_2. *Phys. Chem. Chem. Phys.* **2014**, *16*, 20382–20386.
3. Sheng, Z.; Hu, Y.; Xue, J.; Wang, X.; Liao, W. A novel co-precipitation method for preparation of Mn–Ce/TiO_2 composites for NOx reduction with NH_3 at low temperature. *Environ. Technol.* **2012**, *33*, 2421–2428.
4. Polat, M.; Soylu, A.M.; Erdogan, D.A.; Erguven, H.; Vovk, E.I.; Ozensoy, E. Influence of the sol-gel preparation method on the photocatalytic NO oxidation performance of TiO_2/Al_2O_3 binary oxides. *Catal. Today* **2015**, *241*, 25–32.
5. Hosokawa, M.; Nogi, K.; Naito, M.; Yokoyama, T. *Nanoparticle Technology Handbook*, 1st ed.; Elsevier: Amsterdam, The Netherlands, 2007.
6. Ren, R.; Yang, Z.; Shaw, L.L. Polymorphic transformation and powder characteristics of TiO_2 during high energy milling. *J. Mater. Sci.* **2000**, *35*, 6015–2026.
7. Begin-Colin, S.; Girot, T.; le Caër, G.; Mocellin, A. Kinetics and Mechanisms of Phase Transformations Induced by Ball-Milling in Anatase TiO_2. *J. Solid State Chem.* **2000**, *149*, 41.
8. Pan, X.; Ma, X. Study on the milling-induced transformation in TiO_2 powder with different grain sizes. *Mater. Lett.* **2004**, *58*, 513–515.
9. Pan, X.; Ma, X. Phase transformations in nanocrystalline TiO_2 milled in different milling atmospheres. *J. Solid State Chem.* **2004**, *177*, 4098–4103.
10. Uzunova-Bujnova, M.; Dimitrov, D.; Radev, D.; Bojinova, A.; Todorovsky, D. Effect of the mechanoactivation on the structure, sorption and photocatalytic properties of titanium dioxide. *Mater. Chem. Phys.* **2008**, *110*, 291–298.
11. Billik, P.; Plesch, G.; a, V.B.; Kuchta, L.; Valko, M.; Mazur, M. Anatase TiO_2 nanocrystals prepared by mechanochemical synthesis and their photochemical activity studied by EPR spectroscopy. *J. Phys. Chem. Solids* **2007**, *68*, 1112.
12. Begin-Colin, S.; Gadalla, A.; Cacer, G.L.; Humbert, O.; Thomas, F.; Barres, O.; Villiéras, F.; Toma, L.F.; Bertrand, G.; Zahraa, O.; et al. On the Origin of the Decay of the Photocatalytic Activity of TiO_2 Powders Ground at High Energy. *J. Phys. Chem. C* **2009**, *113*, 16589–16602.
13. Yin, S.; Yamaki, H.; Komatsu, M.; Zhang, Q.; Wang, J.; Tang, Q.; Saito, F.; Sato, T. Preparation of nitrogen-doped titania with high visible light induced photocatalytic activity by mechanochemical reaction of titania and hexamethylenetetramine. *J. Mater. Chem.* **2003**, *13*, 2996–3001.
14. Zhang, Q.; Wang, J.; Yin, S.; Sato, T.; Saito, F. Synthesis of a visible-light active TiO_2-xSx photocatalyst by means of mechanochemical doping. *J. Am. Ceram. Soc.* **2004**, *87*, 1161–1163.
15. Chen, J.; Hirasaki, G.J.; Flaum, M. Effect of OBM on wettability and NMR responses *J. Pet. Sci. Eng.* **2006**, *52*, 161–171.
16. Flood, C.; Cosgrove, T.; Espidel, Y.; Welfare, E.; Howell, I.; Revell, P. Fourier-Transform Carr-Purcell-Meiboom-Gill NMR Experiments on Polymers in Colloidal Dispersions: How Many Polymer Molecules per Particle? *Langmuir* **2008**, *24*, 7875–7880.
17. Madhusudan, B.M.; Raju, H.P.; Ghanaraja, S. Micro Structrual Characterization and Analysis of Ball Milled Silicon Carbide. *AIP Conf. Proc.* **2018**, *1943*, 020122, doi:10.1063/1.5029698.
18. Kim, J.; Chang, J.H.; Jeong, B.Y.; Lee, J.H. Comparison of Milling Modes as a Pretreatment Method for Cellulosic Biofuel Production Hyeon. *J. Clean Energy Technol.* **2013**, *1*, 45–48.
19. Damonte, L.C.; Zelis, L.A.M.; Soucase, B.M.; Fenollosa, M.A.H. Nanoparticles of ZnO obtained by mechanical milling. *Powder Technol.* **2004**, *148*, 15–19.
20. Lemine, O.M.; Louly, M.A.; Al-Ahmari, A.M. Planetary milling parameters optimization for the production of ZnO nanocrystalline. *Int. J. Phys. Sci.* **2010**, *5*, 2721–2729.
21. Molladavoudi, A.; Amirkhanlou, S.; Shamanian, M.; Ashrafizadeh, F. The production of nanocrystalline cobalt titanide intermetallic compound via mechanical alloying. *Intermetallics* **2012**, *29*, 104–109.
22. Lu, K.; Zhao, K.J. Equiaxed zinc oxide nanoparticle synthesis. *Chem. Eng. J.* **2010**, *160*, 788–793.
23. Ozcan, S.; Can, M.M.; Ceylan, A. Single step synthesis of nanocrystalline ZnO via wet-milling. *Mater. Lett.* **2010**, *64*, 2447–2449.
24. Glushenkov, A.M.; Zhang, H.Z.; Chen, Y. Reactive ball milling to produce nanocrystalline ZnO. *Mater. Lett.* **2008**, *62*, 4047–4049.

25. Dulian, P.; Buras, M.; Żukowski, W. Modyfication of photocatalytic properties of titanium dioxide by mechanochemical method. *Polish J. Chem. Technol.* **2018**, *3*, 68–71.
26. Aysin, B.; Ozturk, A.; Park, J. Silver-loaded TiO_2 powders prepared through mechanical ball milling. *Ceram. Int.* **2013**, *39*, 7119–7126.
27. Khan, H.; Swat, I.K. Fe^{3+}-doped Anatase TiO_2 with d–d Transition, Oxygen Vacancies and Ti^{3+} Centers: Synthesis, Characterization, UV–vis Photocatalytic and Mechanistic Studies. *Ind. Eng. Chem. Res.* **2016**, *55*, 6619–6633.